Planetary and Space Science 67 (2012) 57–69

Contents lists available at SciVerse ScienceDirect

Planetary and Space Science

journal homepage: www.elsevier.com/locate/pss

The Biological Oxidant and Life Detection (BOLD) mission: A proposal for a mission to Mars

Dirk Schulze-Makuch [a,*], James N. Head [b], Joop M. Houtkooper [c], Michael Knoblauch [d], Roberto Furfaro [e], Wolfgang Fink [f,g], Alberto G. Fairén [h,p], Hojatollah Vali [i], S. Kelly Sears [i], Mike Daly [j], David Deamer [k], Holger Schmidt [k], Aaron R. Hawkins [l], Henry J. Sun [m], Darlene S.S. Lim [h], James Dohm [n], Louis N. Irwin [o], Alfonso F. Davila [p], Abel Mendez [q], Dale Andersen [p]

[a] School of Earth and Environmental Sciences, Washington State University, Webster Hall 1148, Pullman, WA, United States
[b] Raytheon Missile Systems, Tucson, AZ, United States
[c] Center for Psychobiology and Behavioral Medicine, Justus-Liebig University of Giessen, Germany
[d] School of Biological Sciences, Washington State University, Pullman, WA, United States
[e] Department of Systems and Industrial Engineering, University of Arizona, Tucson AZ, United States
[f] Visual and Autonomous Exploration Systems Research Laboratory, Division of Physics, Mathematics and Astronomy, California Institute of Technology, Pasadena, CA, United States
[g] Department of Electrical & Computer Engineering and Biomedical Engineering Department, University of Arizona, Tucson, AZ, United States
[h] Space Science & Astrobiology Division, NASA Ames, Moffett Field, CA, United States
[i] Department of Earth & Planetary Sciences/Department of Anatomy & Cell Biology, McGill University, Montréal, Québec, Canada
[j] Department of Earth and Space Science and Engineering, York University, Toronto, Ontario, Canada
[k] School of Engineering, University of California Santa Cruz, CA, United States
[l] Electrical and Computer Engineering, Brigham Young University, Provo, UT, United States
[m] Division of Earth and Ecosystem Sciences, Desert Research Institute, Las Vegas, NV, United States
[n] Department of Hydrology and Water Resources, University of Arizona, Tucson, AZ, United States
[o] Department of Biological Sciences, University of Texas at El Paso, TX, United States
[p] Carl Sagan Center for the Study of Life in the Universe, Mountain View, CA, United States
[q] Planetary Habitability Laboratory, University of Puerto Rico at Arecibo, Puerto Rico

ARTICLE INFO

Article history:
Received 20 October 2011
Received in revised form
12 March 2012
Accepted 13 March 2012
Available online 29 March 2012

Keywords:
Mars mission
Viking
Life detection
Oxidant
Microbial life
Instrumentation

ABSTRACT

The next step in the exploration of Mars should include a strong and comprehensive life detection component. We propose a mission called BOLD: Biological Oxidant and Life Detection mission. The scientific objectives of the BOLD mission are to characterize habitability of the martian surface and to search for evidence of extinct or extant life. In contrast to the Viking mission, which was designed to detect heterotrophic life on Mars, the BOLD mission incorporates a more comprehensive search for autotrophic microorganisms, as well as detecting a variety of biomarkers and understanding their environment. Six miniature landers are envisioned for BOLD that utilize either an orbital (e.g. Viking) or direct entry (e.g., MER, Phoenix) mission architecture. The number of landers will provide mission redundancy, and each will incorporate a Mars Soil Analyzer, a Multispectral Microscopic Imager, a Nanopore-ARROW that detects biopolymers with single molecule resolution, an Atmospheric Structure and Surface Environment Instrument, a Fluorescent Stain experiment, and a Chirality experiment. A terrain navigation system, coupled with robust propulsion, permits a landing accuracy on the order of meters if required to meet the science objectives. The probes will use existing orbiters for communication relay if the orbiter architecture proves too ambitious.

1. Introduction

The primary goal of the Viking landers was to conduct life detection experiments on Mars. The consensus view is that Viking did not detect life, but instead observed reactive soil chemistry. This conclusion was based on the evolution of O_2 upon wetting the soil, the apparent absence of organic molecules in the soil, and the weakly positive result of the single control test in the Pyrolytic Release experiment (Klein, 1999). However, recent findings raise questions about the certainty of these interpretations (e.g., Houtkooper and Schulze-Makuch, 2007). For example, a re-analysis indicated that the Viking gas-chromatograph mass spectrometer was much less sensitive than originally assumed, due to interference with minerals in the martian soil among other factors (Navarro-González et al., 2006).

More recent missions that studied the martian surface include the NASA Pathfinder, the Phoenix lander, and the on-going Mars

* Corresponding author. Tel.: +1 509 335 1180; fax: +1 509 335 3700.
E-mail address: dirksm@wsu.edu (D. Schulze-Makuch).

0032-0633/$ - see front matter © 2012 Elsevier Ltd. All rights reserved.
http://dx.doi.org/10.1016/j.pss.2012.03.008

Exploration Rover (MER). Focusing on geology and environmental conditions, these studies are confirming that favorable habitable conditions existed on early Mars, possibly large standing bodies of water (Scott et al., 1995; Fairén et al., 2003; Schulze-Makuch et al., 2008). The next mission to Mars is the NASA Mars Science Laboratory (MSL) which was launched late in 2011. The MSL will test the habitability of Mars, both in regard to possible future human colonization and endemic martian life. The European Space Agency ExoMars mission is planned for launch in 2018. However, since the Urey package (Aubrey et al., 2008) has been dropped from the mission due to budgetary pressures, no currently scheduled future mission contains a life detection component.

Thus, despite past and current missions, the possibility of extant life and biological activity remains an open question. Large deposits of water ice have been found on Mars (Malin and Edgett, 2000; Boynton et al., 2002; Feldman et al., 2002; Mitrofanov et al., 2002), as well as evidence of contemporary liquid water (Malin et al., 2006; McEwen et al., 2011). Methane has been detected in the martian atmosphere, perhaps as a product of biological activity (Formisano et al., 2004; Krasnopolski et al., 2004; Mumma et al., 2004), and there are also indications of contemporary hydrothermal activity (Schulze-Makuch et al., 2007a). The proposed *Biological Oxidant and Life Detection Mission (BOLD)* will search for evidence of biological activity in these martian environments and determine the nature of the unknown oxidizers.

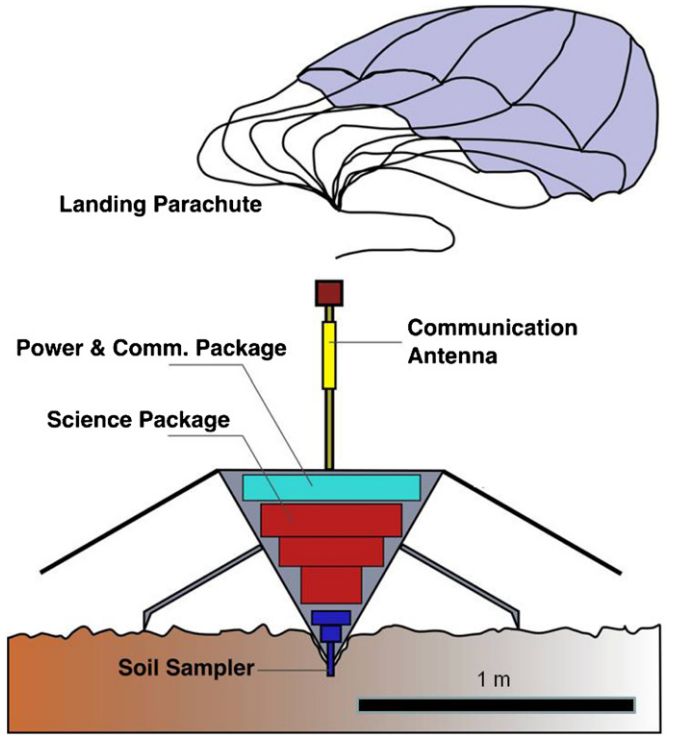

Fig. 1. BOLD probe, schematic overview. Six of these landers are planned to be deployed.

2. General mission design

The BOLD mission will characterize the habitability of the martian surface by searching for oxidants, particularly hydrogen peroxide and perchlorates, and probing for biosignatures near the martian surface (Schulze-Makuch et al., 2007b). The BOLD mission will conduct a more comprehensive search targeting autotrophic microbes, as well as generic biomarkers indicative of the possible presence of life. The mission will carry six probes to provide redundancy in case some of them do not land successfully or fail. A terrain navigation system, coupled with a closed-loop guidance system (Head et al., 2005; Furfaro et al., 2012) and sufficient propulsion capability to correct navigation and guidance errors permits landing precision on the order of 10 m. The probes will require an orbiter for communicating data to Earth. This could be an existing spacecraft such as NASA Mars Reconnaissance Orbiter, ESA Mars Express, or another spacecraft orbiting Mars at that time.

The BOLD mission will use an optical guidance system and employ live telemetry during the descent of the probes. The probes will be powered by batteries and are light-weight, with a science payload of about 7.8 kg, ~10% of the landed mass. The lander system uses a crushable shell behind the heat shield instead of landing gear. The mission duration for each landing probe is anticipated to be a minimum of 2 Sols (martian days), but may be extendable to 10 Sols or more. A schematic view of a landing probe is shown in Fig. 1.

Various designs of the landing probe are under consideration. One possibility is to have the probe in the shape of an inverted pyramid descending on a small parachute for probe orientation and landing velocity control. The envisioned landing conditions are far less stressing than previous missions or concepts (Smrekar et al., 1999; Smith et al., 2011). The impact will push the probe a few tens of centimeters into the martian regolith. After impact, a sampling mechanism (spring-action sampler) will be activated, which both collects and delivers near-surface materials to instruments located in the center of the probe. The sampler will have moisture and temperature sensors, as well as the capability to collect and return material to the interior of the landing probe for further analysis. The hollow-stem penetrator of very narrow diameter could be assisted by a pressurized device (volatile cartridge with regulated pressure). The design of the sampler and of the landing probe will be optimized for the environmental and surface conditions likely to be encountered. The design will be based on tests where pyramidal shape, mass, and impact velocity will be varied to determine on how deep the probe might penetrate under what soil conditions. The sampling mechanism is within current capabilities, but can only be activated once for each probe. The pyramidal design eliminates the need for a drill, but is limited to use on soft sediments rather than rocky materials. Remote imaging of the prospective landing sites such as through the High Resolution Imaging Science Experiment (HIRISE) combined with high precision landing capability will reduce the chances of landing on hard surfaces. The probes' hardiness is determined by prior landing simulations on Earth and by optimizing the design. In addition, the mission risk associated with landing on undesirable surfaces is reduced by probe redundancy: If the probability of landing success for each probe is 50%, the chance that at least one of the probes will succeed is $>98\%$.

3. Previous mission studies involving probes and penetrators

As discussed above, the BOLD mission has been uniquely conceived to deploy a set of six (6) probes equipped with instruments packages for a detailed study of the martian surface habitability. Over the past decades, a few mission concepts for deep space exploration that involve probes and/or penetrators have been proposed and/or flown. In this section, we briefly review three of such mission concepts to highlight similarities and differences with the BOLD mission architecture.

The concept of deploying probes on the martian surface is not new. For example, the ill-fated Mars Polar Lander (MPL) carried

on-board two identical impactors known as Deep Impact A and B. As part of the NASA New Millenium technology demonstration program, the Mars Microprobe Mission (also known as Deep Space 2, Smrekar et al., 1999) piggybacked the two 2.4 kg probes on the MPL cruise stage ring before deployment. The probes had no rockets, parachutes or airbags to decelerate and soften the impact. They were designed to sustain an impact velocity of about 200 m/s with a forebody capable of withstanding without damages a peak acceleration of 30,000*g*'s. The probes were equipped with a descent accelerometer to measure the atmosphere density and an impact accelerometer to estimate the depth of penetration (estimated to be between 0.2 m and 0.6 m). Additional instrument packages were included to acquire a soil sample and heat it to 10 °C to detect potential water vapor. The probes were deployed, but communication was never established.

More recently, LunarNet (Smith et al., 2011) has been proposed as part of the ESA M3 call for medium sized space exploration mission. The mission architecture comprises four penetrators each equipped with a descent module for de-orbiting and attitude control. Each module plus penetrator is assumed to be 51 kg. A single penetrator weights 13 kg and will include a suite of scientific instruments including micro-seismometers, a geochemistry package, a water/volatiles detector, a heat flow experiment, and an impact accelerometer. After a powered de-orbiting, a ballistic phase will follow during which the attitude control re-orient the descent body-fixed camera to image the surface until impact (estimated to be less than 20,000*g*'s).

Gowen at al. (2011) made a case for including penetrators as part of the ESA/NASA Europa Jupiter System Mission. The team proposed a set of two penetrators to (a) provide redundancy, and (b) improve scientific return. The penetrators and their Penetrator Delivery System (PDS) plus a descent camera will comprise the Descent Module (DM). The PDS comprises a solid motor for de-orbiting, a hydrazine tank for attitude control and a set of gyros for attitude sensing. The penetrator mass will range between 5 and 15 kg depending on the instrument suites and will be able to survive up to 20,000*g*'s.

As comparison, the BOLD probes are all equipped with a descent module capable of precision targeting and soft landing (see Mission Architecture section). Consequently, the probes are not impactors and the proposed landing instrument packages (~7.8 kg/probe) do not need to be designed to sustain high impact accelerations.

4. The landing package

The need for miniaturization. As with all space missions, payload mass, size, and power consumption remain the primary concerns and constraints. Miniaturization is especially a concern for the proposed BOLD mission, because the weight constraints for each probe dictates that miniaturization has to be extended down to the component/sensor level. Our strategy for miniaturization is potentially warranting the use of *Micro Electro Mechanical Systems* (*MEMS*) as described in Fink et al. (2007a). MEMS devices, due to their inherently low mass, size, and power, are ideal for both space and sensor network applications. A number of MEMS devices have been specifically developed for the purpose of robotic planetary exploration (George, 2002, 2003; Fink et al., 2007a).

The landing package will include six major experiments related to life and oxidant detection, in addition to a sampler, a battery package, and a transmitter for surface to orbit communication. Several of the experiments require injection and sampling of liquid water, similar to the Viking lander experiments (Klein, 1974, 1977).

4.1. The Mars Soil Analyzer (MSA)

The pyrolytic Gas Chromatograph Mass Spectrometer (GCMS) onboard the 1976 Viking Landers did not provide any evidence of organic compounds on the surface of Mars (Biemann et al., 1977; Biemann, 1979). The commonly advanced explanation for the lack of GCMS results is the presence of one or various potent oxidizing agents in the soil. The Viking Gas Exchange (GEx) and Labeled Release (LR) experiments indicated that the martian soil contains a chemical compound of a highly oxidizing nature (Klein, 1977; Oyama et al., 1977). The GEx experiments showed that the humidification of 1 cm^3 of martian soil sample produced as much as 790 nmol of O_2 gas (Oyama et al., 1977). In the LR experiment, the addition of a radioactive ^{14}C labeled nutrient solution to soil samples resulted in the production of $^{14}CO_2$ due to the breakdown of the organic species introduced (Klein, 1977; Levin and Straat, 1977). These results have been interpreted to be caused by chemical oxidation reactions involving hydrogen peroxide (H_2O_2) and another, less concentrated but thermally stable, oxidant agent (Zent and McKay, 1994). Both oxidants are thought to be produced photochemically in the martian atmosphere, later diffusing into the soil (Hunten, 1979; Bullock et al., 1994). Once in the soil, these oxidants would be stabilized through chemisorption to mineral surfaces (Quinn and Zent, 1999). The low temperatures on the surface of Mars would favor relatively long residence times (Bullock et al., 1994).

Yet the exact nature of the oxidants in the martian soil remains enigmatic. Houtkooper and Schulze-Makuch (2007) proposed a testable alternative hypothesis for the Viking results based on microorganisms that use a metabolism adapted to martian environmental conditions by utilizing hydrogen peroxide as intracellular solvent (referred to as hydrogen peroxide–water hypothesis). Table 1 shows a comparison of the H_2O_2–H_2O hypothesis with conventional chemical explanations. Establishing the type and concentration of oxidants in the martian soil is critical to any future human presence on Mars and for the design of life detection missions. A comprehensive description of the soil is also important to understand its chemical reactivity, effects on organic compounds, and habitability potential. Therefore, we intend to characterize soil samples at each landing site with a suite of chemical, mineralogical, and biological analyses. The analysis of martian soil will be carried out by the Mars Soil Analyzer (MSA), which consists of a small circular apparatus (with a diameter and height of 17 cm and 8 cm, respectively) specially designed to simultaneously carry out two different aqueous chemistry experiments: (1) the Soil Oxidants Experiment (SOE) for the detection of H_2O_2 in the soil; and (2) the Soil Inorganics Experiment (SIE) for the analysis of soil pH, Eh, and inorganic ionic composition (Cl^-, ClO_4^-, Br^-, NO_3^-, K^+, Na^+, Ca^{2+}, Mg^{2+} and NH_4^+).

The Mars Soil Analyzer (MSA) has a circular platform holding ten sample reaction chambers. Each reaction chamber consists of a standard spectrophotometer cuvette of 3.5 ml ($12 \times 12 \times 45$ mm) with a magnetic pill as a mixer (Fig. 2). The magnetic pill is activated by means of a rotating electrical motor with a magnet attached to it, and is used to stir and homogenize the sample within the chamber, if necessary. Each cuvette is equipped with a set of sensors or photoelectrical components specifically chosen for the type of analyses that will be carried out. Based on the electrical components, the theoretical operational temperature of the reaction chamber is −40 °C to 85 °C (optimum −10 °C to 40 °C). A thermoelectric heater will control the reaction chamber temperature. Each experiment will be replicated three times at every landing site to ensure reproducibility of the results.

The presence of H_2O_2 in soil samples will be measured via the leuco crystal violet (LCV) method, originally developed by Mottola et al. (1970). This methodology was recently improved by

Table 1
Explanations for some remaining questions after Viking (modified from Houtkooper and Schulze-Makuch, 2007).

Open question	Chemical explanation	H_2O_2–H_2O hypothesis
Lack of identified organic molecules	The organics have been oxidized to nonvolatile salts of benzenecarboxylic acids, and perhaps oxalic and acetic acid (Benner et al., 2000).	Upon death of the organisms, the organics are spontaneously oxidized by the previously intracellularly bound H_2O_2 with no or very little organic residue. Non-biology bound organic molecules are oxidized chemically (Benner et al., 2000) and/or consumed by organisms. The release of 50–700 ppm of CO_2 by the Viking GC–MS may indicate that oxidation of organic material took place (Navarro-González et al., 2006).
Lack of identified oxidant	There is some yet unidentified mechanism producing H_2O_2 or other oxidants. The oxidant might be present in form of a compound that has no analog on Earth. Suggested inorganic oxidants include metal oxides such as Fe- and Ti-oxides (Quinn and Zent, 1999) and superoxide ions (Yen et al., 2000).	The H_2O_2 in the H_2O_2–H_2O mixture is part of the biochemistry of the putative martian organisms. It would explain the oxidizing potential observed in the Viking results. However, some soil chemistry reactions certainly play a role in the response to the Viking lander experiments as well.
Release and partial resorption of O_2, CO_2, and N_2 in the GEx experiment	Evolution of O_2 on humidification was suggested to involve one or more reactive species such as ozonides, superoxides, and peroxides (Oyama and Berdahl, 1977). CO_2 production in the wet mode can be interpreted to be related to the oxidation of nutrient organic compounds (Oyama et al., 1977), and N_2 release can be interpreted to be related to an initial N_2 desorption from soil by water vapor and subsequent resorption in liquid water (Oyama et al., 1977).	The release of O_2 (and possibly CO_2 to a lesser degree) can be interpreted as the result of an energy-producing metabolism. Upon humidification it could point also to the decomposition of dying martian biota, as could the increase of N_2. The decrease of N_2 can be understood as biological fixation if it exceeded the amount due to physical sorption, a possibility also entertained by Oyama et al. (1977).
Synthesis of organic material in PR experiment	No consistent explanation has been provided, but attempts to explain the observations include instrument malfunction, incorporation of ^{14}CO into carbon suboxide polymer preformed on the martian surface, and reduction of ^{14}CO by H_2O_2 in the surface material (Horowitz et al., 1977).	Some of the putative organisms were able to metabolize and synthesize organic compounds before they died being overwhelmed by water.
Responses in the labeled release experiment	Laboratory tests on Earth using inorganic oxidants and clay minerals simulated many of the key findings, but not the decrease of responses after storage at elevated temperatures (Klein, 1999).	Limited metabolism (Levin and Straat, 1977, 1981) before the organisms died due to hyperhydration, osmotic pressure, and heat shock.

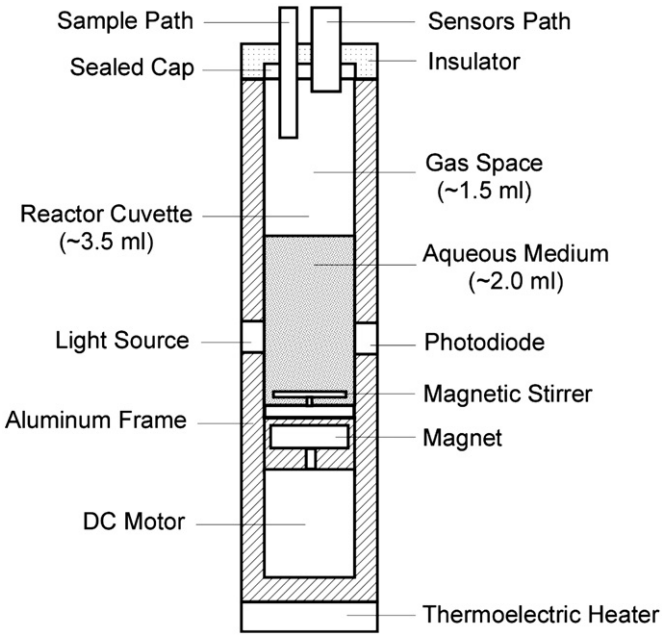

Fig. 2. The Mars Soil Analyzer (MSA) consists of various small reactor modules. Each module has a cuvette that can be adapted to measure various soil properties. A sample aqueous solution of martian soil is injected in the reactor cuvette where a magnetic stirrer keeps the sample homogeneous. Various sensors through the sensors path measure concentration of inorganic ions, pH and Eh. A light sensor and photodiode measures optical density, turbidity or colorimetry (i.e. H_2O_2 concentration) of the sample. A thermoelectric heater controls the temperature of the module.

Cohn et al. (2005) for H_2O_2 detection and quantification in the μM to several hundred nM range in iron-containing solutions with varying pH. The LCV method involves oxidation of 4,4′,4″-methylidynetris in the presence of H_2O_2 and horseradish peroxidase (HRP; see Sternberger et al., 1970) to form the crystal violet ion, CV^+, which absorbs at 590 nm. Calibration curves for pH and the presence of iron have been developed, as the LCV method is strongly affected by pH, with an optimal pH range of 3.6–4.2 (Cohn et al., 2005). Importantly, the colored CV^+ is stable for days, which makes this method independent from immediate access to a spectrophotometer, and thus especially appropriate for martian in situ analyses.

The experiment will begin by collecting surface material with the soil sampler. A small portion of the core sample will be deposited in a reaction chamber. The sample will be mixed in the cuvette with a solution containing a pH buffer 4.2 (H_3PO_4) and the LCV solution, which consists of leuco crystal violet, HRP, and HCl. The cuvette will be opaque, so that the procedure is carried out in the dark. A miniaturized light source on one side of the cuvette will emit at 590 nm through the sample, and a photo-diode on the opposite side of the cuvette will measure the absorbance due to the presence of H_2O_2 (Fig. 2). The same procedure will be repeated in five cuvettes.

The targeted soil inorganic ions for the soil inorganic ion analyses include Cl^-, ClO_4^-, Br^-, NO_3^-, K^+, Na^+, Ca^{2+}, Mg^{2+}, and NH_4^+. Additionally, pH and Eh will also be measured. The analyses will be carried out in five reaction chambers. To that end, a small amount of soil sample will be introduced in the cuvette pre-loaded with a volume of pure liquid water, which will be kept liquid by a thermal element. With the aid of the magnetic pill, the soil will be mixed with the water until a homogeneous solution is obtained. The analysis of the sample is carried out by a small suite of solid-state microsensors located on both sides of the cuvette. Solid state and PVC-membrane based ion selective electrodes could be inherited from the Wet Chemistry Laboratory developed for the Phoenix lander mission (Kounaves et al., 2009), and be adapted to the reaction chambers.

4.2. Multispectral microscopic imager experiment

Minerals that contain water or that can only precipitate from an aqueous solution are potential sites for preserved biosignatures. A microscopic imager (MI) will, therefore, be designed for the BOLD mission to support the in-situ recognition and detection

of both extant and extinct life on Mars. The imager will enable the investigation of biosignatures by imaging rock and mineral particles showing evidence for the presence of water and biogenic material. The resolution (1 to 2 μm) should be sufficient to identify geometric patterns with shapes similar to known terrestrial microfossils in sedimentary rocks, or in the absence of such markers, shapes of biominerals as a possible sign for biological activity. Identifying life unambiguously is tenuous using one observational platform, as shown through the Life in The Atacama Experiment (LITA) (Cabrol et al., 2007), but with multiple lines of evidence, including the MI-based perspective, life could be confirmed remotely, as is the BOLD approach, consistent with the LITA effort. For example, MI will interface with the Fluorescent Stain (FS) Experiment (described in the next section) to yield robust results.

The MI will have up to a 5-mm-wide high-resolution field-of-view, LED light source illumination and a silicon-based imager. A spectral spot photometer is under study for inclusion (see also Fink et al., 2007b). The microscope operates using both reflected LED illumination and background ambient light—should the final lander configuration allow it. The design of the system enables the identification of geometric patterns that may be representative of organic and inorganic materials present as inclusions or as precipitates on rough surfaces and in the fractures of crystalline material. Different combinations of visible and UV light will enable the distinction among evaporite, clay, and carbonate minerals. The application of LED-UV light enables the identification of organic and inorganic components that autofluoresce. Each specific organic molecule has a distinct spectrum; in simple cases, if the peaks on a given UV–visible absorption spectrum are compared to a list of known peaks, it is possible to identify some structural features of an unknown molecule. Many organic molecules have a unique UV absorbance signature. Individual components such as tannic acid, humic acid, or fulvic acid can be identified through their individual absorbance signatures (Birdwell and Engel, 2010). UV-induced fluorescence is important to enhance the detection of biogenic traces. The resolution and detection limit of the MI when combined with other BOLD experiments such as FS is sufficient to resolve individual bacteria and image their content without the need of fluorescent dyes (Table 2).

The high optical resolution restricts the field of view to a few millimeters, so that the microscopic imager must provide contextual views of 10 to 20 mm as well, though at a lower resolution (Fig. 3). This will be accomplished by one of two methods. Two objectives can be switched using a turret. In the past, this would have been the only practical approach but with the miniaturization and integration of imaging systems, it may be that the low mass and low complexity approach is to include two-separate imaging systems and thereby remove the complexity of the moving turret. The major complication of this approach is to configure the system to allow the two cameras, and perhaps the spot spectrometer, to image the same sample area. A system trade is required in conjunction with the sampling device to determine if the sampling device can provide this motion.

Table 2
System requirements of multispectral microscopic imager.

System requirement	Value
Objectives	2, on turret
Resolution	1 μm/20 μm
Depth of field	10 μm/3 mm
Focus extension	Yes
Field of view	1 mm/20 mm
Working distance	20–30 mm
Color	standard pseudo-photopic
Color resolution	12 bit
Illumination	Visible
Fluorescence excitation	240–390 nm
Maneuverability	3D
Mode	Reflective
Sample preparation	External

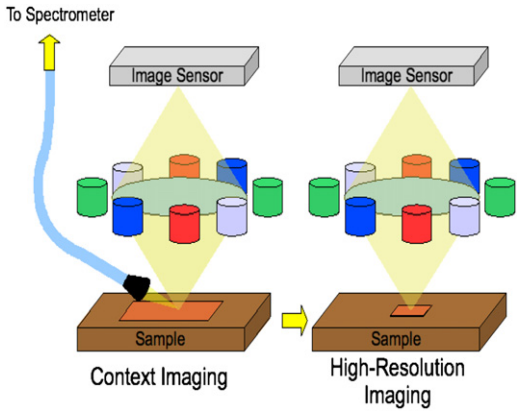

Fig. 3. The microscopic imager is shown schematically in its two configurations. Multi-wavelength light emitting diodes (shown as red, green, blue and violet) illuminate the sample sequentially. The differing fields-of-view in each mode are shown in light-brown with light paths in transparent-yellow. A fiber-optic coupled spectrometer is shown integrated with the context imaging but could be a third imaging station depending on the sampling device capabilities. It is expected that the imaging systems will be ~1 kg with the spectrometer being an additional 500 g.

Light from the sample is imaged onto the sensor, which is converted to digital electrical data. The silicon imager provides an electrical shutter. White-light or red–green–blue LED illumination is necessary in order to be independent of solar lighting and to create shaded areas on rough surfaces. A ring illuminator that is concentric with the lens provides the illumination. The spectrometer is an optimal extension of the functionality of the microscopic imager. It will provide 5 nm resolution over a band of several hundred nanometers. Separating the spectrometer from the microscope optics allows the flexibility of optimizing the band outside of the range of the microscope. For BOLD, strong consideration will be given to providing a longer-wavelength spectrometer capable of identifying hydrated minerals in the 2 to 2.5 μm band (Mustard et al., 2008). According to Rossel and McBratney (1998) the strong absorption bands of the OH groups in soil water are around 1450, 1950, and 2500 nm.

4.3. *The fluorescent stain (FS) experiment*

A major challenge in extraterrestrial microscopic investigations is to discriminate microorganisms from mineral precipitates of comparable shape and size. New state-of-the-art techniques are overcoming this problem. Many fluorescent dyes are polar or ionized, and therefore cannot readily transfer through the barrier of biological membranes. Thus, specific fluorescent dyes have been developed in which an acetate forms an ester bond with the polar residue of the fluorescent dye, turning it into a hydrophobic non-fluorescent molecule that is able to cross the membrane by passive diffusion (Wright et al., 1996; Knoblauch and van Bel, 1998). Once inside the cell, non-specific esterase enzymes cleave the acetate ester bond and convert the substance into a polar fluorescent dye that is now trapped inside the cell (Froelich et al., 2011). As a result, the cells become brightly fluorescent and can easily be distinguished within a large background of non-fluorescent material such as silicaceous soil particles. Esterase enzymes are present within all living organisms on Earth, because

they are involved in numerous metabolic processes. The fluorescent stain procedure described above is now widely used to discriminate between living and dead cells, because dead cells lack esterase activity. Further fluorescent strategies use dyes that stain DNA, such as SYTO 9, while others indicate metabolic activity by sensing redox potentials (e.g. 5-cyano-2,3-ditolyl tetrazolium chloride; CTC). The dyes have superior quantum yield (the ratio of photons absorbed to photons emitted), allowing visualization of sub-micrometer bacterial cells.

A combination of 3 different dyes, all with the same range of excitation and emission wavelength, will be employed to detect possible life forms on Mars. The test chamber will be covered with an appropriate beam splitter to allow excitation of the fluorescent stain and the detection of emitted light. This method will be coupled with the microscopic imager. The laser diode will be used for excitation and the CCD chip for the detection and imaging of possible fluorescent organisms. If kept frozen and in dark, modern dyes can be stored for years, so any problems of instability are not anticipated during the transfer to Mars.

4.4. Nanopore-ARROW biosensor

Given that life on Earth is fundamentally polymeric, it is reasonable to assume that life elsewhere will also choose linear polymers as a structural and functional framework. It follows that life detection could be simplified to a search for linear ionic polymers that have been released into the environment just as nucleic acids are released by many terrestrial microorganisms, either as plasmids or products of hydrolytic degradation. Detecting ionic linear polymers resembling nucleic acids or proteins would provide a strong biosignature for identifying life on Mars. Recent developments in liquid-core optical waveguides allow fabrication of fully planar optofluidic labs-on-a-chip. For this mission, we, therefore, propose to develop a high-performance, low-cost instrument suitable for life detection on planetary surfaces such as Mars. It combines the features of nanopore-based detection with optofluidic ARROW waveguide integration in a unique way, and is called the Nanopore-ARROW (AROPOR) device.

Nanopore-based analysis can characterize single polymer molecules with unmatched speed (micro to millisecond time scale) (Akeson et al., 1999; Storm et al., 2005) and sensitivity (Vercoutere et al., 2001). Not only does this instrument identify individual molecules, but in the process, it captures information about populations of polymeric molecules at rates ranging from a few to hundreds per second. Complete nucleic acids and proteins would not be expected to survive as such in the martian environment, but instead they may be present as fragments or monomers.

Although the speed and sensitivity of a nanopore detector make it a good candidate for powerful new analytical applications, two key elements are needed to make this instrument available for an instrument package to explore a planetary surface such as on Mars. The first is the availability of a robust nanopore sensor. Several different approaches are now available to create nanopores in which inorganic silicon, SiN, SiO_2, or graphene membranes contain a nanoscopic pore (Li et al., 2001; Storm et al., 2005; Garaj et al., 2011).

We have developed synthetic nanopores integrated into a microfluidic chip that could match or surpass hemolysin in detecting and analyzing nucleic acids in solution. Solid state nanopores are mechanically robust, tolerate a broad range of temperatures, pH, and chemical conditions, and have low capacitance, i.e., provide a low-noise surface suitable for integrated electronics. We have developed a two-stage fabrication process for the solid state nanopore that makes it possible to easily control and vary pore dimensions to optimize them for a particular application, e.g., probing single stranded vs. double stranded DNA (Holmes et al., 2010). These nanopores are capable of registering translocation of single biological nanoparticles. For instance, we have recently demonstrated the controlled detection of single 50 S ribosomal sub-units (Rudenko et al., 2011) on a microfluidic chip. In much the same way, DNA molecules can produce characteristic current blockade signals in a solid-state pore of proper size (as they do in the hemolysin pore).

AROPOR life detection instrument: the second key element is an optical single molecule detector that is compatible with the electrical nanopore approach. A new and sophisticated approach to single molecule biosensors utilizes technology associated with the new field of optofluidics that has seen rapid development over the last few years (Psaltis et al., 2006; Monat et al., 2007; Hawkins and Schmidt, 2010; Chen et al., 2011; Kühn et al., 2009a, b, 2010; Schmidt and Hawkins; 2011). We are now in the process of combining nanopore and waveguide technology into an integrated design that takes advantage of both technologies. Because it incorporates a nanopore and an ARROW waveguide, we refer to the device as an AROPOR. The resulting instrument will have a mass of a few hundred grams, and will require electrical power that does not exceed that available on the BOLD mission. This instrument will be unique in its ability to detect biosignatures related to possible microbial life on Mars in the form of ionized polymeric solutes resembling nucleic acids and proteins.

The samples to be investigated are aqueous extracts of martian soil. The amounts required are small, in the range of one gram, and the extraction is performed by mixing the soil with 10 ml of salt solution buffered at pH 8.0. Small aliquots (100 μl) of the filtered extract are then delivered to the AROPOR sample intake. The core sensor technology incorporates a micron-scale ARROW microfluidic compartment (Yin et al., 2004), which is cross-illuminated with exciting light from an LED laser source (Fig. 4). Integrated ARROW waveguides are fabricated in a completely monolithic process that does not require any wafer bonding steps and is fully compatible with conventional complementary metal-oxide-semiconductor (CMOS) fabrication technology (Barber et al., 2006).

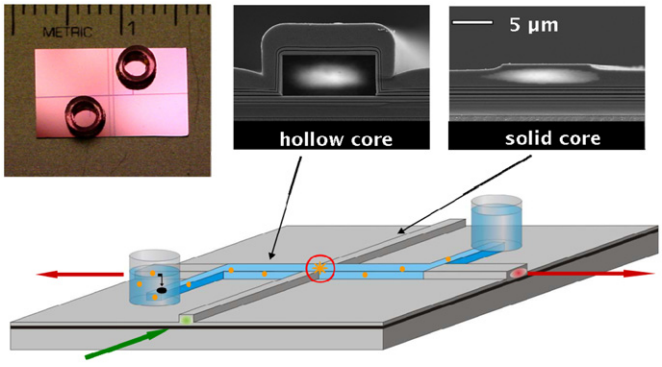

Fig. 4. AROPOR life detection instrument. Optical waveguides with solid (gray) and liquid (blue) cores are fabricated on a silicon chip using standard microfabrication technology. The hollow waveguides are filled with liquid analyte solution, and molecules are introduced into the channel through a nanopore in single file as shown in the figure. The molecules are excited at the solid-hollow waveguide intersection using low-power laser excitation (green arrow). The generated fluorescence signal (red arrows) is captured by the liquid-core ARROW waveguide and directed to the end facet of the chip where it is collected by a lens or optical fiber and routed to a single photon detector. The use of fiber optics and optical waveguides allows the optical detection of single molecules without the need for a bulky, three-dimensional high-resolution microscopy setup. The insets show scanning electron microscope cross sections of the optical waveguides and a photograph of a completed chip, respectively.

ARROWs have been used to demonstrate both single dye molecule fluorescence detection (Yin et al., 2007), as well as detection and analysis of single biological nanoparticles (Yin et al., 2007) and viruses (Rudenko et al., 2009). A nanopore is produced by ion beam sculpting, and is used as a gate to guide single analyte particles into the laser excitation volume. As each particle passes through the illuminated femtoliter volume by electophoretic flow, a fluorescent marker on the particle emits photons, and these are collected by the waveguide and sent via fiber optics to an avalanche photodiode detector (Yin et al., 2006).

The prototype ARROW waveguide device now being tested has a volume of 0.1 m^3 and a mass of $\sim$5 kg. The power requirements are minimal, on the order of tens of milliamps for the sensor and microfluidics. However, there are no technical barriers to reducing mass, volume and power requirements to that of a cell phone. A recent example of miniaturization technology is the February 2012 announcement by Oxford Nanopore Technologies that they will market a hand-held nanopore-based sequencing device for $900. (See their website for details.)

4.5. The Chiral Detection (CD) experiment

The Viking Labeled Release (LR) experiment indicated that martian topsoil can degrade labile organics (Klein et al., 1976). At both landing sites fresh soil rapidly gave off $^{14}CO_2$ upon addition of an aqueous nutrient solution containing ^{14}C-labeled organic molecules (formate, glycolate, glycine, D- and L-alanine, and D- and L-lactate). Although the response is consistent with heterotrophic metabolism, a biological interpretation was rejected in order not to contradict another Viking experiment, pyrolysis-gas chromatography–mass spectrometry (pyr-GC–MS), which failed to detect indigenous organics at the level of parts per billion (Klein, 1977; Klein, 1978). The most widely held explanation for the LR activity is that martian soil contains one or more photochemical oxidants, such as hydrogen peroxide. However, recent studies questioned the detection limit of the pyr-GC–MS. The pyrolysis temperature used, 500 °C, may not have been high enough to recover all organics (Benner et al., 2000) and the high iron content of martian soil may have interfered, resulting in an underestimation of the organic content (Navarro-González et al., 2006). pyr-GC–MS may not be sensitive enough to detect a bacterial population of 10^6 cells per gram soil (Glavin et al., 2001). These insights compel a revisit to the question of a native soil biota on Mars.

The BOLD mission will conduct a new generation LR capable of differentiating chemical and biological reactivity. Labile organic compounds will be added to soil in pure enantiomers. Chemical oxidants are expected to destroy both D- and L-isomers. In contrast, microorganisms would be selective and consume only one enantiomer. This experiment is non-Earth-centric and would detect life forms that are based on either isomer. The concept has been validated with glucose and terrestrial microorganisms (Rudney, 1940, Sun et al. 2009). The BOLD Chiral Detection experiment could borrow heavily from the Viking legacy in terms of hardware design to minimize mission cost.

4.6. Meteorological payload and environmental sensors

The Viking, Pathfinder and Phoenix landers featured meteorology sensors that recorded temperature, pressure, and wind velocity during descent and at the landing sites. Each lander in the BOLD mission will be equipped with an identical suit of sensors to conduct atmospheric and environmental measurements. The BOLD atmospheric structure and surface environment instrument (ASSEI) will operate during entry and descent, and after landing. During entry, at an approximate altitude of 125 km, atmospheric density will be measured with accelerometers. Controlled descent will occur at approximately 12 km. From there to the surface, atmospheric temperature and pressure will also be measured by each lander. One of the main features of the proposed mission is its redundancy with six probes that will land at different martian localities. This will allow for the first time to obtain up to six atmospheric profiles of these parameters from approximately 12 km altitude down to the surface at different latitudes and longitudes. The main objectives of these measurements are (1) to determine the three-dimensional structure of the atmosphere, and (2) to understand the global atmospheric circulation system.

Table 3
Suite of environmental sensors.

Sensor	Rationale	Previous missions
Atmospheric pressure	Global climate/water stability	√
Atmospheric temperature	Global climate/habitability/ water stability	√
UV radiation	Habitability/soil chemistry	√
Wind speed and direction	Global climate/habitability/eolian processes	√
Atmospheric RH	Global climate/habitability/ soil chemistry/water stability	√
PAR	Habitability	X
Acoustic sound	Public outreach	X

One of the key objectives of the BOLD mission is to search for extant martian life on and near the surface. As such, a suite of sensors capable of recording different environmental parameters at each landing site is a key component. If BOLD succeeds in finding evidence for, or strong indications of extant martian life, data obtained from the environmental sensors would provide valuable information about the conditions in which these organisms live, and would help us understand their survival strategies. If, on the contrary, BOLD is unable to find any evidence or indication of life, the environmental data will still aid in defining the habitability conditions of both the surface and near-surface of Mars. Each lander will be equipped with a suite of environmental sensors as listed in Table 3. Once on the surface, each lander will record high-resolution time series of the atmospheric temperature, relative humidity (RH), pressure, wind velocity and direction, photosynthetic active radiation (PAR), UV irradiation, and acoustic sound. The sensors will be operative for a minimum of 2 Sols and perhaps up to 10 Sols or longer, and will acquire 6 data points per hour in order to provide excellent resolution of hourly and daily perturbations of these environmental parameters. Detailed atmospheric temperature and RH data will result in an improved understanding of the daily water vapor dynamics and the stability of water near the surface. Both PAR and UV radiation data are fundamental to assessing the habitability of the martian surface, having significant bearing on the design of future missions to the planet. Wind velocity and direction data are necessary to understand near-surface eolian processes such as slope winds, convective cells, or dust devils. A microphone is also planned to be incorporated into the meteorological payload and environmental sensors. There is still no record of acoustics on the martian surface, despite several attempts on previous missions (i.e., Mars Polar Lander, Beagle 2, Williams (2001)). Microphones deployed at the potential six landing sites would provide a strong public outreach component, drawing the public closer to the exploration of Mars.

4.7. Onboard data processing, analysis, and anomaly detection

The above mentioned instruments of the BOLD lander payload have to be interfaced with and controlled by an onboard (sensor)

data acquisition, data analysis, and anomaly detection system. This system will not only control the experiments, read out and analyze the sensor data, but will also provide the resulting processed data packages to the onboard transceiver system for uplink to an orbiter for further relay to Earth. Due to the high ionic and UV irradiation flux on the surface of Mars, each lander probe will be equipped with a rad-hardened embedded computer system. At the core of the data processing, data analysis, and anomaly detection, a modified and customized version of the *Automated Global Feature Analyzer* (*AGFA*; for details see Fink et al., 2005, 2008) will be deployed. AGFA is a first-of-a-kind approach towards a fully automated and comprehensive characterization of an operational area. Although currently focused mainly on geologic classification, future extensions of AGFA will address (1) geophysical, (2) geochemical, (3) (hyper-)spectral, and (4) biological classifications of operational areas for enhanced geologic and exobiological exploration.

AGFA performs automated feature extraction, classification, anomaly detection, and target prioritization within mapped operational areas at different length scales and resolutions (e.g., microscopic images of soil samples provided by the microscopic imager). For example, in the *geologic* operation mode, AGFA comprehensively extracts features, such as target shape, size, color, albedo, texture, vesicularity, angularity, eccentricity, compactness, extent, and thereby obtains *feature vectors* for the identified targets within the imaged operational area. These feature vectors are subsequently used by AGFA to summarize the mapped operational area numerically, to classify targets, and to automatically flag anomalies, i.e., targets that exhibit sufficient anomalous character within the instrument–inherent feature space(s) as opposed to user/scientist bias. The raw instrument/sensor data and the extracted numeric feature vectors together with their classification and anomaly detection, provided by AGFA, can be uplinked to an orbiter via the onboard transceiver for further relay to Earth.

5. Mission architecture

The mission architectures considered for BOLD have similarities to and significant differences from those approaches normally employed in penetrator missions (e.g. Smith et al., 2011; Gowen et al., 2011). In such cases, the descent module will employ an initial powered phase for de-orbiting, followed by a ballistic (unguided) entry, followed by a guided phase to drive the individual probe towards the target, then a final unguided, parachute-retarded, descent to the surface.

Two mission architectures are being considered at this initial level of analysis. The first is exemplified by the Viking mission, in which the landers were carried to Mars by a cruise stage that maneuvered into martian orbit, adjusted the orbit based on landing site selection, and eventually deployed the lander. For the BOLD mission using this architecture, the landers would be deployed one-by-one to the desired landing locations. This permits near-global access, in which each lander could be individually targeted at different landing sites. In reality, orbiter performance will limit the landing locations, most likely in latitude. This architecture is not dependent on other Mars orbiting assets for communications relay. This approach is similar to that described for LunarNet (Smith et al., 2011).

The second architecture, called direct entry, has been used by all NASA missions since Viking. The cruise stage makes no effort to enter Mars orbit, being limited to refining the trajectory such that the landers will enter the martian atmosphere safely and touch down within the landing ellipse. Based on past missions these are typically 20 km × 100 km at best (the Mars Science Laboratory is expected to improve that to 20 km × 20 km). However, it is highly desirable for this mission to employ terrain-aided navigation (e.g. Head et al., 2005) to achieve a pinpoint landing. In this case the expected landing error is on the order of ~10 m. There may be a limited ability to target the landers separately at the cost of mission complexity and risk, but even so the dispersion of landing sites would be small, likely on the order of 1000 km or less. The relative merits of the orbiter and direct entry architectures are summarized in Table 4.

Table 4
Comparison of parameters for orbiter and direct entry mission architecture.

Parameter	Orbiter	Direct entry
Vehicle mass	~2900 kg	~1500 kg
Launch vehicle	Atlas V 421 class (30% margin)	Atlas V 401 class (80% margin)
Surface science	Global access	Regional access (~1000 km)
Operations	Sustained in Mars orbit	Minimum
Critical events	All DI events+MOI, trims	TCMs, Lander deployments

5.1. Analysis of the basic mission parameters

In the following, mission parameters are discussed in sufficient detail for interested readers to understand the complexities involved in planning a Mars lander mission. A preliminary analysis of the basic design parameters has been conducted to determine the feasibility of the proposed mission. Such analysis involves various aspects of the overall baseline mission including cruise, Mars orbit and entry, descent, and landing (EDL). A baseline lander concept design has been completed, documenting vehicle mass, power, and communications. Focusing on a single lander of the overall cluster, the baseline mission consists of a sequence of distinct phases:

(a) Cruise phase mass and propulsion capability.
(b) Mars orbit insertion (MOI, if that is the chosen architecture).
(c) Probe deployment and insertion into an atmospheric entry path.
(d) EDL sequence.
(e) Initiation of lander science phase.

The approach taken in this analysis is to start with the science instrument suite, incorporate earlier efforts to develop a design, then determine the propulsion requirements for MOI and cruise. This will set the mass for the cruise stage/orbiter, and hence, the launch mass of the vehicle, which in turn will constrain plausible launch vehicles for this mission.

5.2. Design of spacecraft

Lander: a rudimentary lander design has been devised, consistent with the design of the science payload and based on previous work (e.g., Head et al., 2005, Head et al., 2011). For this work, a science payload mass of 7.8 kg (6 kg current best estimate plus 30% margin) is envisioned. The navigation and attitude determination system uses radiation-tolerant, off-the-shelf components for the star tracker and Inertial Measurement Unit (IMU). While the notional command and data handling employ Broad Reach electronics (Broad Reach Engineering, 2010), communications use the Comtech AeroAstro S-band system to minimize mass and power draw (Comtech AeroAstro, 2010). The aeroshell and structure masses are scaled from the designs of previous Mars landers. This means that the aeroshell would share limited heritage with previous missions and would require significant

design, development, and testing. The thermal control mass assumes that the probe is partially buried in the regolith, i.e., insulated, and makes use of instrument and electronics waste heat. The power system is a primary battery sufficient to run for 2 Sols. Additional landed lifetime can be gained through trading payload or system reserve mass for battery mass. For 10 Sols and 10 kg of primary battery, the average power use would be ~15 W assuming a primary battery with 400 W-hr/kg. MEMS technology permits allocation of <5 W to the instrument payload.

A liquid bi-propellant propulsion system is assumed, as was used on Viking and Mars Observer. In accordance with NASA mission proposal guidelines, a 30% margin is carried throughout, bringing the estimated lander wet mass to 112 kg, including a system reserve on top of the 30% margin. The propulsion system has sufficient Δv during EDL to provide ~10–15 km divert capability to effect a pinpoint landing. This requires that the propagated entry precision be 10–15 km, something not achieved on Mars to date, but close to the advertised precision of MSL. This propulsive capability enables pinpoint landing on the order of 10 m. In order to enter the martian atmosphere, each lander will need to slow its orbital velocity by ~100–200 m/s, based on the Viking lander concept of operations (AGU, 1977). Using a Star-6B solid rocket motor reduces the lander speed by ~140 m/s (ATK, 2007).

If the landing error ellipse is greater than the lander divert capability, then the lander may not reach the desired target. This can be mitigated by denoting multiple suitable science targets

Table 5
Estimate of the Mars-bound mass.

Orbital deployment		Direct entry	
Cruise stage	600 kg	Cruise stage	600 kg
Propellant	1578 kg	Propellant	193 kg
Landers	750 kg	Landers	680 kg
Total	2928 kg	Total	1473 kg

Table 6
Launch capability to Mars by launch date for the Atlas (AV) and Delta (D4) family of boosters. There are many viable options over a range of C3 requirements.

Launch	C3	AV401	AV411	AV501	AV511	D4 Med	D4M (4,2)
2016	8.0	2850	3750	2550	3450	>2350	>3450
2018	7.7	2800	3800	2600	3500	>2350	>3450
2020	13.2	2550	3300	2300	3050	<2350	<3450

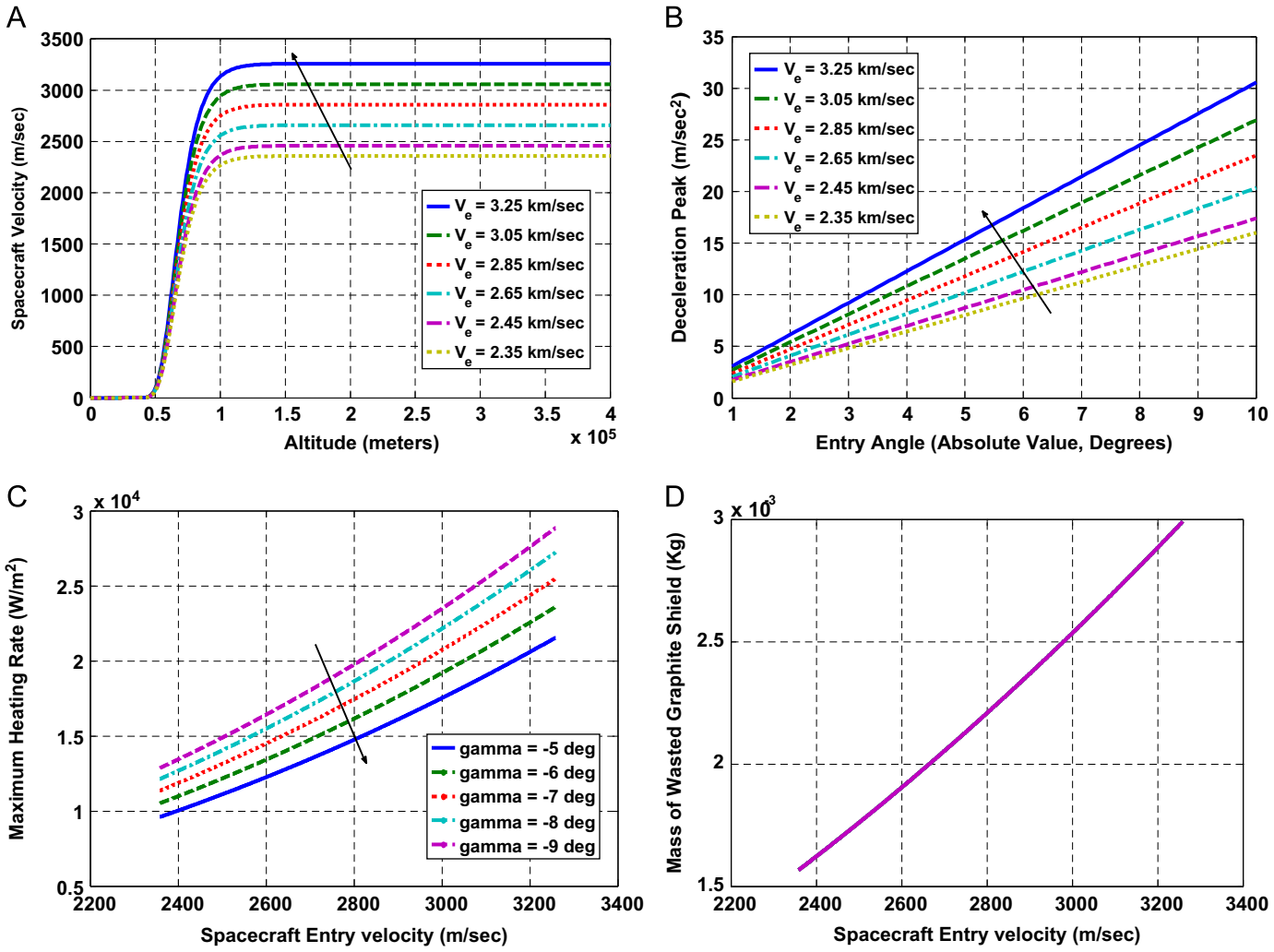

Fig. 5. A first order analysis has been applied to determine the maximum deceleration and to compute the total heat absorbed by the flight vehicle during the entry phase. (A) Altitude–velocity profile during entry phase as function of the entry spacecraft velocity; (B) maximum deceleration experienced by the probe during descent as function of the entry angle; (C) maximum heating rate; (D) mass of graphite shield evaporating as function of the entry spacecraft velocity. The total absorbed heat is estimated to be 10^6 J while the maximum heating rate is estimated to have an upper value of 28 kW/m^2. In case of ablation shielding, graphite high heat of evaporation (10^7 J/kg) is such that only a few grams of the shield evaporate during the entry phase.

within the landing ellipse, so that the lander can continue automatically to the nearest desired landing site once the heat shield and aeroshell are jettisoned. Real-time detection of science targets is enhanced by equipping the overall system with algorithms for intelligent interpretation of data acquired during the descent phase. Intelligent systems based on fuzzy logic (Furfaro et al., 2008, 2010, 2012) and the Automatic Global Feature Analyzer (AGFA, Fink et al., 2005, 2008) have been devised to support such complex tasks. Both software packages can be customized to suit the needs of the BOLD mission.

Cruise Stage/Orbiter: The cruise stage/orbiter must support the six small landers, the propulsion for trajectory correction maneuvers during cruise, and propulsion for the Mars Orbit Insertion (MOI) burn in the orbiter architecture. In addition, the cruise stage/orbiter would carry out all communications to Earth during the cruise stage. The relay of data from the landers during the science mission may rely on other Mars orbiting spacecraft if the direct entry architecture is chosen. Cruise stages and orbiters for previous Mars missions range in mass from ~200 kg (Mars Pathfinder) to ~880 kg (Viking). For BOLD a cruise stage dry mass of 600 kg is assumed.

Based on published data for the MRO, the cruise stage must provide 400 m/s for trajectory correction maneuvers and 1800 m/s for the MOI burn. The MOI burn is sufficient to put the vehicle into an elliptical orbit, relying on aerobraking to circularize the orbit if desired as was done on MRO. The fuel required for the MOI maneuver is the main difference in mass for the two architectures. These considerations determine the cruise stage wet mass and total vehicle launch mass, for which a bi-propellant propulsion system as used on Viking (AGU, 1977) is envisioned. This is summarized in Table 5.

Launch Vehicle: the booster must deliver the BOLD vehicle to a Mars trajectory, the energy of which is characterized by C3, a measure of the payload's specific kinetic energy. C3 varies considerably with launch opportunities, from 7.7 km^2/s^2 in 2018 to 13.2 km^2/s^2 in 2020 (George and Kos, 1998). It appears that a launch vehicle similar to the Atlas V 401 would be adequate for boosting the BOLD vehicle with a direct entry architecture. The orbiter architecture is more massive and would require a larger vehicle such as the Atlas V 421 (Lockheed-Martin Corporation, 2004). The Delta II does not appear to have sufficient lift for this mission; the Delta IV Medium (Boeing, 2004a) and the Delta IV Medium+(4,2) (Boeing, 2004b) have adequate lift for the direct entry and orbital mission architectures, respectively (Table 6). Results of a first order analysis to determine the maximum deceleration and to compute the total heat absorbed of the flight vehicle during the entry phase are shown in Fig. 5.

Payload communication analysis: a link budget design study has been performed to evaluate how much power is required to efficiently transmit data from the landing package to an orbiter. The relationship between transmitting power, data rate, and length of the propagation path and antenna size needs to be defined to perform such a link analysis. The desired relationship is known in the literature as the Link Equation (Wertz and Larson, 1999), and it is useful in computing the Signal-to-Noise-Ratio (SNR also indicated as E_b/N_0 where E_b is the energy per bit [J] and N_0 is the noise spectral density [W/Hz]) as a function of the design parameters:

$$\frac{E_b}{N_0} = \frac{PL_lG_tL_sL_aG_r}{kT_sR} \quad (1)$$

At the numerator, P is the transmitting power, L_l, L_s and L_a are the transmitter-to-antenna, space, and transmission path losses, respectively, and G_t and G_r are the gain of the transmitting and

Table 7
Parameters used in BOLD uplink budget design.

Power range	1–10 W	Range of interest
Data rate range	10 bps–100 kbs	Range of Interest
Frequency	2 GHz	S-Band
Bit error rate	10^{-5}	Typical telemetry
Average distance	600 km	Distance probe-orbiter
Antenna Gain (max)	0.6 dB	Half-way dipole antenna
Atmospheric losses	0 dB	1st order approximation
Polarization losses	0 dB	1st order approximation
Pointing losses	0 deg.	Isotropic antenna
Receiver noise temperature	125 K	From Magellan mission
Spacecraft temperature	100 K	From Magellan mission
Receiving antenna gain	5.6 dB	Medium gain antenna
Modulation index	78 deg.	Typical arrangement

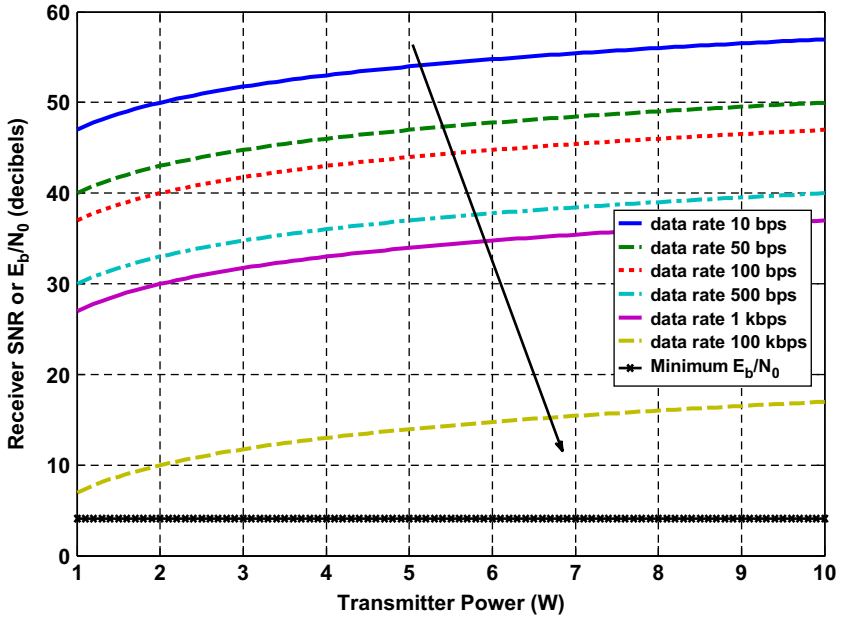

Fig. 6. Signal-to-Noise-Ratio (SNR) as a function of the transmitted power with variable data rate. The black line indicates the required SNR (or E_b/N_0, see text) to guarantee the Bit Error Rate (BER) to be less than 10^{-5}, which is a typical requirement for deep-space missions (e.g., Magellan mission, see "Magellan space final report", Lockheed Martin, MGN-MA-011, Denver, CO, January 1995). Note that the transmitted power refers to what is generally called RF output power.

receiving antennas, respectively. At the denominator, k is the Boltzmann constant, T_s is the system noise temperature, and R is the desired data-rate.

The design parameters used in a preliminary analysis of the transmission uplink (one-way communication probe-to-orbiter is assumed) are listed in Table 7. Fig. 6 shows the Signal-to-Noise Ratio (SNR) as a function of the transmitted power with the data rate as a parameter. Assuming a target Bit Rate Error (BER) of 10^{-5} (unitless), the value of the minimum SNR required to maintain data transmission within the error limits is estimated to be 4.10 dB. It is apparent that 1 W of power is sufficient to transmit data at rates up to 1 kbits/s with a link margin greater than 10 dB. If a higher data rate is required (100 kbps), the transmission data margin is maintained with 5 W of transmitting power. The carrier link margin (i.e., the power margin of the carrier required to provide adequate power for transmission) is also sufficient for efficient transmission (Fig. 7). Importantly, the computed transmitting power is referred to as the RF power output (Wertz and Larson, 1999). The DC input power to be transmitted is generally higher. If the probe employs solid-state transmitters (which are generally preferred for power outputs up to 5 or 10 W), the DC power input power is estimated to vary in the range of 15 W (for 1 W of RF output power) to 30 W (for 5 W of RF output power). The projected mass of the solid-state transmitter is estimated to be 0.5 kg. If a Traveling Wave Tube Amplifier (TWTA) is employed in the transmitting hardware, the DC input power ranges from 10 to 15 W and the estimated transmitter mass between 1 and 2 kg.

6. Targeted landing sites

There are engineering constraints and scientific priorities associated with potential landing sites. The engineering constraints are

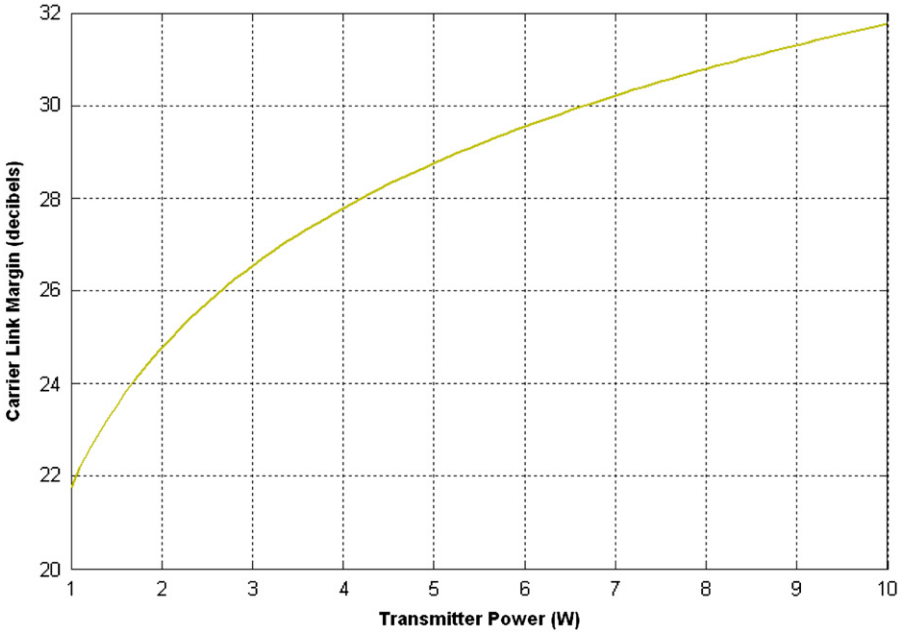

Fig. 7. Carrier link margin as a function of the transmitted power. As in Fig. 2, the transmitted power refers to the RF output power.

Table 8
Summary of instrument payload on BOLD mission.

Instrument/Experiment	Instrument/Experiment description
Mars soil analyzer	Designed to comprehensively describe the type and concentration of oxidants in the martian soil as well as to establish the chemical reactivity and habitability of the martian soil. The emphasis of the Mars soil analyzer instrument will be to detect H_2O_2 in the martian soil and to analyze soil pH, Eh, and inorganic ionic composition. In addition, a suite of environmental sensors will be carried on the BOLD mission to evaluate environmental conditions near the martian surface.
Multispectral microscopic imager	Designed to support the in-situ recognition and detection of both extant and fossilized life (i.e., microfossils) in sedimentary and non-sedimentary rocks as well as biominerals as proxy for biological activity.
Fluorescent stain experiment	Designed to detect biochemistry as known from Earth organisms based on the presence of esterases.
Nanopore-ARROW experiment	Recent developments in nanopore analysis of macromolecules and liquid-core optical waveguides have the potential to allow fabrication of fully planar optofluidic labs-on-a-chip. Nanopores are able to detect single molecules of biopolymers such as DNA and proteins. Liquid-core antiresonant reflecting optical (ARROW) waveguides also have this capability. The novel Nanopore-ARROW instrument combines the strengths of both approaches for life detection on planetary surfaces such as Mars.
Chirality experiment	Labeled release experiment (similar to Viking) capable of differentiating chemical and biological reactivity. Labile organic compounds will be added to soil as pure enantiomers. Chemical oxidants are expected to destroy both D- and L-isomers. In contrast, microorganisms would be selective and consume only one enantiomer. This experiment is non-Earth-centric and would detect life forms that are based on either D- or L-isomers. However, the assumption that Earth organisms consume L-amino acids, not D-amino acids, has yet to be vigorously tested.
Atmospheric Structure and Surface Environment Instrument (ASSEI)	Will record temperature, pressure, and wind velocity during descent and at the landing sites. This environmental data will aid in defining and interpret the habitability conditions of the martian surface around each of the landers.

mostly related to having the BOLD probes impact into softer sedimentary material to secure soil samples that can be tested for oxidants and possible life, and thus BOLD can go to geologic terrains that are otherwise difficult to reach such as the vast canyons system of Mars, Valles Marineris, or the ancient mountain ranges on Mars such as the Thaumasia highlands (Dohm et al., 2001). The scientific priorities are to find promising sites that are (or were) habitable to life, and where active or fossilized life can be recovered. Thus, high-priority targets are (1) certain locations within the polar regions of Mars such as Chasma Borealis due to a high preservation potential in ice and geological activity; (2) locations with elevated heat flow where hydrothermal activity may be present (e.g., Schulze-Makuch et al. 2007a; Dohm et al., 2008); (3) locations where liquid water on Mars may be stable and that have not been explored yet. One example is the canyon bottom of Valles Marineris, where fog may be present (Möhlmann et al., 2009). Fog, for example, is significant to life in the extremely arid desert environments of the Atacama Desert of Chile (e.g., Warren-Rhodes et al., 2007); and (4) locations where phyllosilicates were identified, because these deposits point to liquid water in ancient martian history (Bibring et al., 2005) and preserve organic material well. Workshops are anticipated to be held where the latest insights about possible landing sites will be reviewed, and a priority list will be established.

7. Conclusions

Future missions to Mars, such as the proposed *Biological Oxidant and Life Detection Mission* (*BOLD*), should have a strong life detection component. For BOLD, a non-Earth-centric astrobiological instrument suite will be deployed. The instrument suite is designed to both characterize the oxidant content of martian soil and undertake a comprehensive search for a variety of biomarkers. Even if the BOLD mission is unable to detect biomarkers, the mission will significantly increase our knowledge of the near-surface habitability of Mars. A summary of the proposed instrument suite aboard each of the 6 BOLD landers and how it will increase our knowledge about Mars is presented in Table 8.

References

AGU, 1977. Scientific results of the Viking mission. Journal of Geophysical Research 82, 3959–4681.

Akeson, M., Branton, D., Kasianowicz, J.J., Brandin, E., Deamer, D.W., 1999. Microsecond time-scale discrimination among polycytidylic acid, polyadenylic acid, and polyuridylic acid as homopolymers or as segments within single RNA molecules. Biophysical Journal 77, 3227–3233.

A.T.K., 2007. Space Products Catalog, 223.

Aubrey, A.D., Chalmers, J.H., Bada, J.L., Grunthaner, F.J., Amashukeli, X., Willis, P., Skelley, A.M., Mathies, R.A., Quinn, R.C., Zent, A.P., Ehrenfreund, P., Amundson, R., Glavin, D.P., Botta, O., Barron, L., Blaney, D.L., Clark, B.C., Coleman, M., Hofmann, B.A., Josset, J.L., Rettberg, P., Ride, S., Robert, F., Sephton, M.A., Yen, A., 2008. The Urey instrument: an advanced in situ organic and oxidant detector for Mars exploration. Astrobiology 8 (3), 583–595.

Barber, J.P., Lunt, E., George, Z., Yin, D., Schmidt, H., Hawkins, A.R., 2006. Integrated hollow waveguides with arch-shaped cores. Photonics Technology Letters 18, 28.

Benner, S.A., Devine, K.G., Matveeva, L.N., Powell, D.H., 2000. The missing organic molecules on Mars. Proceedings of the National Academy of Sciences U.S.A 97, 2425–2430.

Bibring, J.P., Langevin, Y., Gendrin, A., Gondet, B., Poulet, F., Berthé, M., Soufflot, A., Arvidson, R., Mangold, N., Mustard, J., Drossart, P., the OMEGA team, 2005. Mars surface diversity as revealed by the OMEGA/Mars Express observations. Science 307, 1576–1581.

Birdwell, J.E., Engel, A.S., 2010. Characterization of dissolved organic matter in cave and spring waters using UV–vis absorbance and fluorescence spectroscopy. Organic Geochemistry 41, 270–280.

Boynton, W.V., et al., 2002. Distribution of hydrogen in the near-surface of Mars: evidence for subsurface ice deposits. Science 297, 81–85.

Biemann, K., Oro, J., Toulmin, P., Orgel, L.E., Nier, A.O., Anderson, D.M., Simmonds, P.G., Flory, D., Diaz, A.V., Rushneck, D.R., Biller, J.E., Lafleur, A.L., 1977. The search for organic substances and inorganic volatile compounds in the surface of Mars. Journal of Geophysical Research 82, 4641–4658.

Biemann, K., 1979. The implications and limitations of the findings of the Viking Organic Analysis Experiment. Journal of Molecular Evolution 14, 65–70.

Boeing, 2004a. Delta II Technical Summary, 6.

Boeing, 2004b. Delta IV Technical Summary, 6.

Broad Reach Engineering, 2010. Command and Data Handling Product Data Sheet. Accessible from 〈http://www.broadreachengineering.com/cdh.html〉.

Bullock, M., Stoker, C.R., McKay, C.P., Zent, A.P., 1994. A coupled soil-atmosphere model of H_2O_2 on Mars. Icarus 107, 142–154.

Cabrol, N.A., Wettergreen, D.S., Warren-Rhodes, K., Grin, E.A., Moersch, J., Chong Diaz, G., Cockell, C.S., Coppin, P., Demergasso, C., Dohm, J.M., Ernst, L., Fisher, G., Glasgow, J., Hardgrove, C., Hock, A.N., Jonak, D., Marinangeli, L., Minkley, E., Ori, G.G., Piatek, J., Pudenz, E., Smith, T., Stubbs, K., Thomas, G., Thompson, D., Waggoner, A., Wagner, M., Weinstein, S., Wyatt, M., 2007. Life in the Atacama: searching for life with rovers (science overview). Journal of Geophysical Research 112 (G04S02)http://dx.doi.org/10.1029/2006JG000298.

Chen, M.M., Eberle, E.J., Lunt, S., Liu, K., Leake, M.I., Rudenko, A.R., Hawkins, Schmidt, H., 2011. Dual-color fluorescence cross-correlation spectroscopy on a planar optofluidic chip. Lab on Chip 11, 1502–1506.

Cohn, C.A., Pak, A., Strongin, D., Schoonen, M.A., 2005. Quantifying hydrogen peroxide in iron-containing solutions using leuco crystal violet. Geochemical Transactions 6, 47–51.

Comtech AeroAstro, 2010. S-Band radio product data sheet. Accessible from 〈http://www.aeroastro.com/datasheets/S-Band_Radio.pdf〉.

Dohm, J.M., Tanaka, K.L., Hare, T.M., 2001. Geologic map of the Thaumasia region of Mars. US Geological Survey Map, I-2650.

Dohm, J.M., et al., 2008. Recent geological and hydrological activity on Mars: the Tharsis/Elysium corridor. Planetary and Space Science 56, 985–1013.

Fairén, A.G., Dohm, J.M., Baker, V.R., de Pablo, M.A., Ruiz, J., Ferris, J.C., Anderson, R.C., 2003. Episodic flood inundations of the northern plains of Mars. Icarus 165, 53–67.

Feldman, W.C., et al., 2002. Global distribution of neutrons from Mars: results from Mars Odyssey. Science 297, 75–78.

Fink, W., Datta, A., Dohm, J.M., Tarbell, M.A., Jobling, F.M., Furfaro, R., Kargel, J.S., Schulze-Makuch, D., Baker, V.R., 2008. Automated global feature analyzer — a driver for tier-scalable reconnaissance. Aerospace Conference, 2008 IEEE, pp.1–12, 1–8 March 2008, doi: http://dx.doi.org/10.1109/AERO.2008.4526422.

Fink, W., Datta, A., Baker, V., 2005. AGFA: (Airborne) Automated Geologic Field Analyzer. Geochimica et Cosmochimica Acta 69 (10S), A535.

Fink, W., George, T., Tarbell, M.A., 2007a. Tier-scalable reconnaissance: the challenge of sensor optimization, sensor deployment, sensor fusion, and sensor interoperability. Proceeding of SPIE. SPIE 6556, 655611, doi: http://dx.doi.org/10.1117/12.721486.

Fink, W., Mahaney, W.C., Kuhlman, K.R., 2007b. Adapter-based Microscopic and Wide-angle Imaging Capability For Digital Cameras For Planetary Exploration and Astrobiology. [abstract 2397]. In: 38th Lunar and Planetary Science Conference Abstracts [CD-ROM]. Lunar and Planetary Institute, Houston.

Formisano, V., Atreya, S., Encrenaz, T., Ignatiev, N., Giuranna, M., 2004. Detection of methane in the atmosphere of Mars. Science 306, 1758–1761.

Froelich, D.F., Mullendore, D.L., Jensen, K.H., Ross-Elliott, T.J., Anstead, J.A., Thompson, G.A., Pelissier, H.C., Knoblauch, M., 2011. Phloem ultrastructure and pressure flow: SEOR protein agglomerations do not affect translocation. Plant Cell 23, 4428–4445.

Furfaro, R., Dohm, J.M., Fink, W., Kargel, J.S., Schulze-Makuch, D., Fairén, A.G., Ferré, P.T., Palmero-Rodriguez, A., Baker, V.R., Hare, T.M., Tarbell, M., Miyamoto, H.H., Komatsu, G., 2008. The Search for life beyond earth through fuzzy expert systems. Planetary and Space Science 56, 448–472.

Furfaro, R., Kargel, J.S., Lunine, J.I., Fink, W., Bishop, M.P., 2010. Identification of cryovolcanism on titan using fuzzy cognitive maps. Planetary and Space Science 5, 761–779.

Furfaro, R., Fink, W., Kargel, J.S., 2012. Autonomous real-time landing site selection for Venus and Titan using evolutionary fuzzy cognitive maps. Applied Soft Computing, doi: http://dx.doi.org/10.1016/j.asoc.2012.01.014. It is available online as of March 20, 2012: http://www.sciencedirect.com/science/article/pii/S1568494612000403.

George, L.E., Kos, L.D., 1998. Interplanetary mission design handbook: Earth-to-Mars mission opportunities and Mars-to-Earth return opportunities 2009–2024. NASA T, M–1998-208533.

George, T., 2002. MEMS/NEMS development for space applications at NASA/JPL. Proceedings of the SPIE 4755, 556.

George, T., 2003. Overview of MEMS/NEMS technology development for space applications at NASA/JPL. Proceedings of the SPIE 5116, 136.

Garaj, S., Hubbard, W., Reina, A., Kong, J., Branton, D., Golovchenko, J.A., 2011. Graphene as a subnanometre trans-electrode membrane. Nature 467, 190–193.

Glavin, D.P., Schubert, M., Botta, O., Kminek, G., Bada, J.L., 2001. Detecting pyrolysis products from bacteria on Mars. Earth and Planetary Science Letters 185, 1–5.

Gowen, R.A., Smith, A., Fortes, A.D., Barber, S., Brown, P., Church, P., Collinson, G., Coates, A.J., Collins, G., Crawford, I.A., Dehant, V., Chela-Flores, J., Griffiths, A.D., Grindrod, P.M., Gurvits, L.I., Hagermann, A., Hussmann, H., Jaumann, R., Jones, A.P., Joy, K.H., Karatekin, O., Miljkovic, K., Palomba, E., Pike, W.T., Prieto-Ballesteros, O., Raulin, F., Sephton, M.A., Sheridan, S., Sims, M., Storrie-Lombardi, M.C., Ambrosi, R., Fielding, J., Fraser, G., Gao, Y., Jones, G.H., Kargl, G., Karl, W.J., Macagnano, A., Mukherjee, A., Muller, J.P., Phipps, A., Pullan, D., Richter, L., Sohl, F., Snape, J., Sykes, J., Wells, N., 2011. Penetrators for in situ subsurface investigations of Europa. Advances in Space Research 48, 725–742.

Hawkins, A.R., Schmidt, H., 2010. Handbook of Optofluidics. CRC Press, Taylor & Francis.
Head, J.N., Hoppa, G.V., Gardner, T.G., Seybold, K.G., Svitek, T., 2005. Autonomous low-cost precision lander for lunar exploration. 36th Lunar and Planetary Science Conference. Abstract #1471.
Head, J.N., Hoppa, G.V., Garner, T.G., Tsetsenskos, K., Dolfini, S., Svitek, T., 2011. United States Patent #7,967,255.
Holmes, M.R., Rudenko, M., Measor, P., Shang, T., Schmidt, H., Hawkins, A.R., 2010. Micropore and nanopore fabrication in hollow arrow waveguides. Journal of Micro/Nanolithography, MEMS, and MOEMS 9, 023004.
Horowitz, N.H., Hobby, G.L., Hubbard, J.S., 1977. Viking on Mars: the Viking carbon assimilation experiments. Journal of Geophysical Research 82, 4659–4662.
Houtkooper, J.M., Schulze-Makuch, D., 2007. A possible biogenic origin for hydrogen peroxide on Mars: the Viking results reinterpreted. International Journal of Astrobiology 6, 147–152.
Hunten, D.M., 1979. Possible oxidant sources in the atmosphere and surface of Mars. Journal of Molecular Evolution 14, 71–78.
Klein, H.P., et al., 1976. The Viking biological investigation: preliminary results. Science 194, 99–105.
Klein, H.P., 1974. Automated life detection experiments for the Viking Mission to Mars. Origins of Life 5, 431–441.
Klein, H.P., 1977. The Viking biological investigation: general aspects. Journal of Geophysical Research 3482, 4677–4680.
Klein, H.P., 1978. The Viking biological experiments on Mars. Icarus 34, 666–674.
Klein, H.P., 1999. Did Viking discover life on Mars? Origins of Life and Evolution of Biosphere 29, 625–631.
Knoblauch, M., van Bel, A.J.E., 1998. Sieve tubes in action. Plant Cell 10, 35–50.
Kounaves, S.P., et al., 2009. The MECA Wet Chemistry Laboratory on the 2007 Phoenix Mars Scout Lander. Journal of Geophysical Research 114 (E00A19). http://dx.doi.org/10.1029/2008JE003084.
Krasnopolski, V.A., Maillard, J.P., Owen, T.C., 2004. Detection of methane in the martian atmosphere: evidence for life? Icarus 172, 537–547.
Kühn, S., Lunt, E.J., Philips, B.S., Hawkins, A.R., Schmidt, H., 2010. Ultralow power trapping and fluorescence detection of single particles on an optofluidic chip. Lab Chip 10, 189.
Kühn, S., Measor, P., Lunt, E.J., Phillips, B.S., Deamer, D.W., Hawkins, A.R., Schmidt, H., 2009a. Loss-based optical trap for on-chip particle analysis. Lab on Chip 9, 2212.
Kühn, S., Measor, P., Lunt, E.J., Phillips, B.S., Hawkins, A.R., Schmidt, H., 2009b. Optofluidic particle concentration by a long-range dual-beam trap. Optics Letters 34, 2306–2308.
Levin, G.V., Straat, P.A., 1977. Recent results from the Viking labeled release experiment on Mars. Journal of Geophysical Research 82, 4663–4667.
Levin, G.V., Straat, P.A., 1981. A search for a nonbiological explanation of the Viking labeled release life detection experiment. Icarus 45, 494–516.
Li, J., Stein, D., McMullan, C., Branton, D., Aziz, M.J., Golovchenko, J.A., 2001. Ion-beam sculpting at nanometre length scales. Nature 412, 166–169.
Lockheed-Martin Corporation, 2004. Atlas launch system payload planners guide, January 2007 revision. 401 pp.
Malin, M.C., Edgett, K.S., 2000. Evidence for recent groundwater seepage and surface runoff on Mars. Science 288, 2330–2335.
Malin, M.C., Edgett, K.S., Posiolova, L.V., McColley, S.M., Noe Dobrea, E.Z., 2006. Present-day impact cratering rate and contemporary gully activity on Mars. Science 314, 1573–1577.
McEwen, A.S., Ojha, L., Dundas, C.M., Mattson, S.S., Byrne, S., Wray, J.J., Cull, S.C., Murchie, S.L., Thomas, N., Gulick, V.C., 2011. Seasonal flows on warm Martian slopes. Science 333, 740–743.
Mitrofanov, I., Anfimov, D., Kozyrev, A., Litvak, M., Sanin, A., Tret'yakov, V., Krylov, A., Shvetsov, V., Boynton, W., Shinohara, C., Hamara, D., Saunders, R.S., 2002. Maps of subsurface hydrogen from the high-energy neutron detector, Mars Odyssey. Science 297, 78–81.
Möhlmann, D.T.F., Niemand, M., Formisano, V., Savijärvi, H., Wolkenberg, P., 2009. Fog phenomena on Mars. Planetary and Space Science 57, 1987–1992.
Monat, C., Domachuk, P., Eggleton, B.J., 2007. Integrated optofluidics: a new river of light. Nature Photonics 1, 106–114.
Mottola, H., Simpson, B.E., Gorin, G., 1970. Absorptiometric determination of hydrogen peroxide in submicrogram amounts with Leuco Crystal Violet and peroxidase as catalyst. Analytical Chemistry 42 (410–411), 1970.
Mumma, M.J., DiSanti, M.A., Novak, R.E., Bonev, B.P., Dello Russo, N., Hewagama, T., Smith, M., 2004. Detection and mapping of methane and water on Mars. American Astronomical Society, DPS meeting #36. Bulletin of the American Astronomical Society. 36, pp. 1127.
Mustard, J., et al., 2008. Hydrated silicate minerals on Mars observed by the Mars Reconnaissance Orbiter CRISM instrument. Nature 454, 305–309.
Navarro-González, R., et al., 2006. The limitations on organic detection in Mars-like soils by thermal volatilization-gas chromatography–MS and their implications for the Viking results. Proceedings of the National Academy of Sciences USA 103, 16089–16094.
Oyama, V.I., Berdahl, B.J., 1977. The Viking gas exchange experiment results from Chryse and Utopia surface samples. Journal of Geophysical Research 82, 4669–4676.
Oyama, V.I., Berdahl, B.J., Carle, G.C., 1977. Preliminary findings of the Viking gas exchange experiment and a model for martian surface chemistry. Nature 265, 110–114.
Psaltis, D., Quake, S.R., Yang, C., 2006. Developing optofluidic technology through the fusion of microfluidics and optics. Nature 442, 381–386.
Quinn, R.C., Zent, A.P., 1999. Peroxide-modified titanium dioxide: a chemical analog of putative Martian soil oxidants. Origins of Life and Evolution of Biospheres 29, 59–72.
Rossel, R.A.V., McBratney, A.B., 1998. Laboratory evaluation of a proximal sensing technique for simultaneous measurement of soil clay and water content. Geoderma 85, 19–39.
Rudenko, M.I., Kühn, S., Lunt, E.J., Deamer, D.W., Hawkins, A.R., Schmidt, H., 2009. Ultrasensitive Qβ phage analysis using fluorescence correlation spectroscopy on an optofluidic chip. Biosensors and Bioelectronics 24, 3258–3263.
Rudenko, M.I., Holmes, M.R., Ermolenko, D.N., Lunt, E.J., Gerhardt, S., Noller, H.F., Deamer, D.W., Hawkins, A., Schmidt, H., 2011. Controlled gating and electrical detection of single 50S ribosomal subunits through a solid-state nanopore in a microfluidic chip. Biosensors and Bioelectronics 29, 34–39.
Rudney, H., 1940. The utilization of L-glucose by mammalian tissues and bacteria. Science 92, 112–113.
Schmidt, H., Hawkins, A.R., 2011. The photonic integration of non-solid media using optofluids. Nature Photonics 5, 598–604.
Schulze-Makuch, D., Dohm, J.M., Fan, C., Fairén, A.G., Rodriguez, J.A.P., Baker, V.R., Fink, W., 2007a. Exploration of hydrothermal targets on Mars. Icarus 189, 308–324.
Schulze-Makuch, D., Houtkooper, J.M., Knoblauch, M., Furfaro, R., Fink, W., Fairén, A.G., Vali, H., Head, J.N., Lim, D.S.S., Dohm, J., Irwin, L.N., Daly, M., Andersen, D., 2007b. The Biological Oxidant and Life Detection (BOLD) Mission: an outline for a new mission to Mars. Proceedings of the SPIE, vol. 6694; b 66940O, 10.1117/12.732155.
Schulze-Makuch, D., Fairén, A.G., Davila, A.F., 2008. The case for life on Mars. International Journal of Astrobiology 7, 117–141.
Scott, D.H., Dohm, J.M., Rice, J.W., 1995. Map of Mars showing channels and possible paleolake basins. USGS Miscellaneous Investigations Series Map, I–2461. (1:30,000,000).
Smith, A., Crawford, I.A., Gowen, R.A., Ambrosi, R., Anand, M., Banerdt, B., et al., 2011. Lunar Net—a proposal in response to an ESA M3 call in 2010 for a medium sized mission. Experimental Astronomy. http://dx.doi.org/10.1007/s10686-011-9250-5.
Smrekar, S., Catling, D., Lorenz, R., Magalhaes, J., Moersch, J., Morgan, P., Murphy, J., Murray, B., Presley-Holloway, M., Yen, A., Zent, A., Blaney, D., 1999. Deep Space 2: the Mars microprobe mission. Journal of Geophysical Research 104 (E11), 27013–27030.
Sternberger, L.A., Hardy Jr., P.H., Cuculis, J.J., Meyer, H.G., 1970. The unlabeled antibody enzyme method of immunohistochemistry: preparation and properties of soluble antigen–antibody complex (horseradish peroxidase–antihorseradish peroxidase) and its use in identification of spirochetes. Journal of Histochemistry and Cytochemistry 18, 315–333.
Storm, A.J., Storm, C., Chen, J., Zandbergen, H., Joanny, J.F., Dekker, C., 2005. Fast DNA translocation through a solid-state nanopore. Nano Letters 5, 1193–1197.
Sun, H.J., Saccomanno, V., Hedlund, B.P., McKay, C.P., 2009. Stereo-specific glucose consumption may be used to distinguish between chemical and biological reactivity on Mars: a preliminary test on Earth. Astrobiology 9, 443–446.
Vercoutere, W., Winters-Hilt, S., Olsen, H., Deamer, D.W., Haussler, D., Akeson, M., 2001. Rapid discrimination among individual DNA molecules at single nucleotide resolution using a nanopore instrument. Nature Biotechnology 19, 248–250.
Warren-Rhodes, K., et al., 2007. Searching for microbial life remotely: satellite-to-rover habitat mapping in the Atacama Desert, Chile. Journal of Geophysical Research 112 (G04S05). http://dx.doi.org/10.1029/2006JG000283.
Wertz, J.R., Larson, W.J., 1999. 3rd ed.Space Mission Analysis and Design, volume 8. Space Technology Library.
Williams, J.-P., 2001. Acoustic environment of the Martian surface. Journal of Geophysical Research 106, 5033–5041. http://dx.doi.org/10.1029/1999JE001174.
Wright, K.M., Horobin, R.W., Oparka, K.J., 1996. Phloem mobility of fluorescent xenobiotics in *Arabidopsis* in relation to their physicochemical properties. Journal of Experimental Botany 47, 1779–1787.
Yen, A.S., Kim, S.S., Hecht, M.H., Frant, M.S., Murray, B., 2000. Evidence that the reactivity of the Martian soil is due to superoxide ions. Science 289, 1909–1912.
Yin, D., Barber, J.P., Hawkins, A.R., Deamer, D.W., Schmidt, H., 2004. Integrated optical waveguides with liquid cores. Applied Physics Letters 85, 3477–3479.
Yin, D., Barber, J.P., Deamer, D.W., Hawkins, A.R., Schmidt, H., 2006. Single-molecule detection sensitivity using planar integrated optics on a chip. Optics Letters 31, 2136–2138.
Yin, D., Lunt, E.J., Rudenko, M.I., Deamer, D.W., Hawkins, A.R., Schmidt, H., 2007. Planar optofluidic chip for single particle detection, manipulation, and analysis. Lab on Chip 7, 1171.
Zent, A.P., McKay, C.P., 1994. The chemical reactivity of the Martian soil and implications for future missions. Icarus 108, 146–157.